

The $\text{FA}_{1-x}\text{MA}_x\text{PbI}_3$ System: Correlations among Stoichiometry Control, Crystal Structure, Optical Properties, and Phase Stability

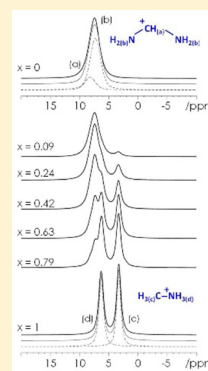
Ambra Pisanu,[†] Chiara Ferrara,[†] Paolo Quadrelli,[†] Giorgio Guizzetti,[‡] Maddalena Patrini,[‡] Chiara Milanese,[†] Cristina Tealdi,[†] and Lorenzo Malavasi^{*,†}

[†]Department of Chemistry and INSTM, University of Pavia, Viale Taramelli 16, Pavia 27100, Italy

[‡]Department of Physics and CNISM, University of Pavia, Via Bassi 6, Pavia 27100, Italy

Supporting Information

ABSTRACT: The $\text{FA}_{1-x}\text{MA}_x\text{PbI}_3$ solid solution has been carefully investigated in terms of the MA/FA stoichiometry, crystal structure, and optical properties. This work allowed for the determination of reliable correlations between the amount of protonated amine and the physicochemical properties. The deleterious effect of aging on the mixed MA/FA composition was observed by diffraction and optical measurements, showing progressive phase separation within the samples.



INTRODUCTION

Mixed methylammonium/formamidinium (MA/FA) lead halide hybrid perovskites have recently attracted significant interest because of the very high efficiencies of perovskite solar cells (PSCs) employing such semiconductor layers, which exhibit strong band-gap photoabsorption.¹⁻⁴ One of the reasons for using these mixed systems is the need to stabilize the black phase (α) of formamidinium lead iodide (FAPbI₃) at room temperature. In fact, at room temperature, FAPbI₃ crystallizes in a hexagonal yellow phase (δ -phase) in the space group $P6_3mc$, whereas the perovskite α -phase, with an optimal band gap of about 1.47–1.49 eV, is achieved by crossing the phase transition above 165 °C.⁵ The black α -phase crystallizes in a cubic symmetry with space group $Pm\bar{3}m$. Interest in the use of FAPI-based perovskites is also related to the facts that (i) the larger FA cation leads to more symmetric perovskites than for the MAPbI₃ (MAPI) phase (which is tetragonal at room temperature), (ii) the smaller band gap of FAPI allows for near-IR absorption, and (iii) perovskites containing FA cations have improved stability.⁶ Most of the solid solutions investigated so far are based on FAPI systems with partial substitution of Br for the I halogen and mixed MA/FA lead iodides.¹⁻⁶ The present work focuses on the latter system.

The $\text{FA}_{1-x}\text{MA}_x\text{PbI}_3$ system has been the subject of a number of studies in the past few years reporting very high efficiencies for PSCs employing such phases.^{2,3,6-8} For example, Pellet et al.² explored several compositions of the $\text{FA}_{1-x}\text{MA}_x\text{PbI}_3$ system using samples prepared in the form of films by infiltrating TiO₂ with PbI₂, dripping these films in mixed FAI and MAI solutions,

and then performing a thermal treatment. According to the observed XRD patterns, each of the samples still contained a significant amount of PbI₂, no lattice parameters were provided, and only relative shifts from the peaks of FAPI were reported. In addition, the starting FAPI sample consisted of a mixture of α and δ phases with a band-gap value, E_g , for pure FAPI reported to be 1.530 eV, which is higher than most of the values reported in the current literature (about 1.48 eV). Moreover, the E_g values reported for phases with very different nominal stoichiometries, such as FAPbI₃ and $\text{FA}_{0.4}\text{MA}_{0.6}\text{PbI}_3$, were the same.² Such anomalous trends might be due to the peculiar growth kinetics of the films prepared by the reported method, leading to a difference between the nominal and real compositions. In the work of Binek et al., XRD investigation on powdered samples revealed the stabilization of the cubic phase of FAPI when the amount of FA was greater than 20%, whereas for lower stoichiometries, the solid solution maintained the tetragonal symmetry of MAPI.⁶ The authors also reported no lattice shrinkage upon the replacement of about 13% of the FA with MA and confirmed the stabilization of the α -phase induced by MA doping already at relatively low amounts. Moreover, in ref 6, for all of the levels of MA doping in α -FAPI (5%, 10%, and 15% MA), the band gap remained the same, at about 1.52 eV.⁶ A very recent work by Jacobsson et al. presented a comprehensive investigation of the $\text{FA}_{1-x}\text{MA}_x\text{PbI}_3$ system.³ In that case, the band-gap value of FAPI was reported 43

69 to be 1.52 eV, the trend of the cell volume as a function of MA
70 content did not follow a linear trend (as predicted by Vegard's
71 law for solid solutions), and no information was provided on
72 the real stoichiometries of the prepared films. It is surprising to
73 see how large the spread is in the reported results for the
74 $\text{FA}_{1-x}\text{MA}_x\text{PbI}_3$ system in terms of the crystal structure and
75 optical properties. Some of the discrepancy might arise from
76 the presence of powdered and thin-film samples and, for the
77 latter, from the fact that their preparation by means of different
78 routes can lead to compositions that differ from the nominal
79 ones. Another relevant point might be the actual phase stability
80 of FA-rich phases. Concerning this last point, the literature does
81 not provide any information about the time stability of the α -
82 phase within the $\text{FA}_{1-x}\text{MA}_x\text{PbI}_3$ system. It is well-known that
83 the pseudocubic black phase of pure FAPI can be stabilized at
84 room temperature after a thermal treatment of the hexagonal
85 phase above 165 °C, but that this phase, being a metastable
86 phase, progressively converts to the yellow phase with time.⁵ A
87 very recent work addressed the structural behavior of this solid
88 solution and found that the cubic perovskite phase is stable up
89 to $x = 0.8$, whereas the mixed phase is tetragonal for higher
90 stoichiometries. No information has been provided about the
91 phase stability of mixed phases, even though express mention is
92 made of the fact that pure FAPI is not stable in the perovskite
93 phase.⁹

94 Considering the significant interest in the $\text{FA}_{1-x}\text{MA}_x\text{PbI}_3$
95 mixed system related to the high efficiencies of the PSCs
96 employing such materials as absorbers, in the present article, we
97 report a detailed investigation of the crystal structure, optical
98 properties, and phase stability of this solid solution as a
99 function of x carried out on samples with well-defined cation
100 stoichiometries (i.e., x values), as determined by NMR
101 spectroscopy.

102 ■ EXPERIMENTAL METHODS

103 **Material Preparation.** Samples of general formula
104 $\text{FA}_{1-x}\text{MA}_x\text{PbI}_3$ were synthesized according to a general
105 procedure that we developed previously.^{10,11} In a typical
106 synthesis, a proper stoichiometric amount of lead acetate is
107 dissolved in excess HI under continuous mechanical stirring
108 under a nitrogen atmosphere. Then, the solution was heated to
109 100 °C, and the corresponding amines (methylammonium
110 and/or formamidinium in water, 40 wt %) were added in the
111 correct stoichiometric amounts. The solution was then cooled
112 to 46 °C at 1 °C/min, until the formation of a precipitate,
113 which was immediately filtered and dried under a vacuum at 60
114 °C overnight. All reagents were purchased from Sigma-Aldrich
115 in pure form and were used without any further purification.

116 **X-ray Diffraction.** The crystal structures of the samples
117 were characterized by room-temperature Cu-radiation Powder
118 X-ray diffraction (XRD) on a Bruker D8 diffractometer. Scans
119 were performed in the 10–90° range, with a step size 0.02° and
120 a counting time of 8 s/step. Data were fitted by the Rietveld
121 method using the FullProf suite of programs.¹²

122 **Diffuse Reflectance Measurements.** The optical diffuse
123 reflectance spectra of the different perovskites were measured
124 from 0.8 to 4.5 eV (250–1500 nm, in steps of 1 nm) on a
125 Varian Cary 6000i spectrophotometer equipped with an
126 integrating sphere. For this type of measurement, polycrystal-
127 line powders were compacted into pellets of about 10 mm in
128 diameter, and reflectance spectra were calibrated using a
129 standard reference disk.

NMR Spectroscopy. ¹H solid-state NMR room-temper-
130 ature spectra were acquired on a 9.4 T (¹H = 400.16 MHz)
131 Bruker Avance III spectrometer with the use of TopSpin 3.1
132 software; spectra were collected with a 4-mm magic-angle-
133 spinning (MAS) probe under 8 kHz spinning conditions. ¹H
134 quantitative one-pulse experiments were performed with a
135 pulse length of 4.65 μs, a recycle delay of 120, and 16 scans.
136 The pulse length and recycle delay were carefully calibrated
137 before the acquisition of the final spectra to ensure the full
138 relaxation of the magnetization and to fulfill the conditions for
139 quantitative data acquisition. Chemical shifts are referred to
140 tetramethylsilane (TMS) using adamantane as a secondary
141 standard. The analysis of the obtained data was performed
142 using the DMFit program.¹³

Differential Scanning Calorimetry (DSC). DSC measure-
144 ments were performed in a Q2000 apparatus from TA
145 Instruments by heating about 25 mg of powder from –90 to
146 200 °C in Al open crucibles under a flux of nitrogen.
147

148 ■ RESULTS AND DISCUSSION

149 Samples synthesized according to the experimental procedure
150 were first investigated by solid-state ¹H NMR spectroscopy to
151 determine their *actual* FA/MA ratios. ¹H MAS spectra for the
152 whole $\text{FA}_{1-x}\text{MA}_x\text{PbI}_3$ series are reported in Figure 1, together
153 with the corresponding attributions and the best fits for the two
154 end members.

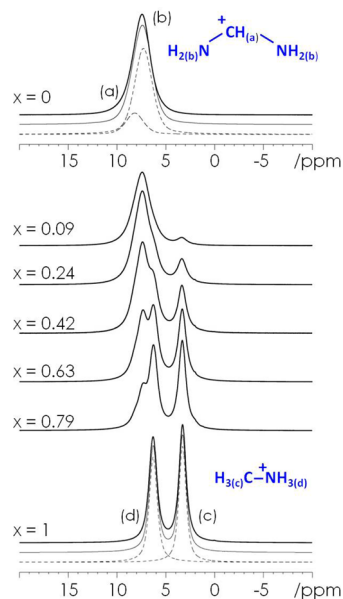


Figure 1. Solid-state NMR spectra of the $\text{FA}_{1-x}\text{MA}_x\text{PbI}_3$ solid solution. Dashed lines represent fit contributions, and the light solid line represents the overall best fit to the experimental spectra.

The spectrum of the FAPI composition presents two peaks at 155 7.53 and 8.87 ppm with a relative ratio of 4:1, and these signals
156 can be attributed to the $-\text{NH}_2$ and $-\text{CH}$ protons, respectively.
157 Similar chemical shifts were observed for the NMR signal
158 (liquid) of the $\text{HC}(\text{NH}_2)_2\text{I}$ and FAPI precursors used for the
159 synthesis of FAPI.^{7,14} Similarly, the attribution of the MAPI
160 composition was made considering the presence of the two
161 resonances at 6.22 and 3.28 ppm with a ratio of 1:1. These two
162 signals have been previously correlated with the $-\text{NH}_3^+$ and
163 $-\text{CH}_3$ protons, respectively, of the series MAPbX_3 ($X = \text{I}, \text{Br},$
164 Cl).¹⁵ The signals of the two MA and FA species were only 165

166 partially overlapping, and at the experimental MAS speed (8
 167 kHz), the observed lines were sufficiently sharp and the
 168 acquisition parameters (pulse length and recovery delay) were
 169 optimized to obtain fully relaxed signals. Under these
 170 conditions, the quantitative analysis of the mixed samples was
 171 possible, and the results are reported in Table 1.

Table 1. Nominal Composition and Composition Determined from Analysis of ^1H NMR Spectra for the $\text{FA}_{1-x}\text{MA}_x\text{PbI}_3$ Series^a

FA/MA ratio	
nominal	NMR-determined
1.0:0.0 ($x = 0$, pure FAPI)	1.0:0.0
0.8:0.2	0.91:0.09
0.7:0.3	0.76:0.24
0.5:0.5	0.58:0.42
0.3:0.7	0.37:0.63
0.1:0.9	0.21:0.79
0.0:1.0 ($x = 1$, pure MAPI)	0.0:1.0

^aBest-fit error < 5%.

172 Analysis of the NMR data revealed that the actual
 173 compositions of the samples were slightly different from the
 174 nominal compositions used for the synthesis (see the
 175 [Experimental Methods](#) section), as the MA amount was always
 176 slightly overestimated. This result suggests that proper control
 177 of the actual MA/FA ratio for this and related systems is a key
 178 aspect to be checked after material synthesis, also considering
 179 that most of the synthetic procedure is carried out in solution
 180 by dripping methods where a proper control of precursor
 181 stoichiometry might be hard to achieve. A possible origin of the
 182 difference between the nominal and measured stoichiometries
 183 might be the different solubilities/reactivities of the MA and FA
 184 precursors in solution.

185 ^1H and ^{13}C solid-state NMR techniques have been exploited
 186 for the study of the phase transitions between different
 187 polymorphs for MA lead halide perovskites series,¹⁵ whereas
 188 ^1H liquid NMR data for mixed MA/FA iodide precursors have
 189 been presented to confirm the alloying of MA and FA in MA-
 190 stabilized FAPI.¹⁴ Nevertheless, to our knowledge, this is the
 191 first time that ^1H solid-state NMR spectroscopy has been used
 192 to address the problem of the quantitative determination of
 193 mixed FA/MA compositions. Based on the NMR results, the x
 194 values in the $\text{FA}_{1-x}\text{MA}_x\text{PbI}_3$ solid solution (within the
 195 estimated standard deviations) were 0, 0.09, 0.24, 0.42, 0.63,
 196 0.79, and 1.0.

197 The X-ray diffraction (XRD) patterns of all of the samples
 198 investigated in the present work are reported in [Figure 2](#).

199 All of the samples were single-phase, and for those from $x =$
 200 0 to $x = 0.79$, the unit cell was in agreement with the crystal
 201 structure of the α -phase (black perovskite) of the FAPI end
 202 member. In the inset of [Figure 2](#), the XRD pattern of FAPI is
 203 compared with the literature reference pattern using the $Pm\bar{3}m$
 204 space group, and this black sample was obtained by annealing
 205 the yellow, as-synthesized, FAPI sample at 185 °C for 1 h. On
 206 the other hand, MAPI has a diffraction pattern consistent with
 207 the reported tetragonal structure in the $I4mc$ space group.¹⁰
 208 The reported patterns show similar peak shapes and small full
 209 width at half-maximum (fwhm) as well, indicating good
 210 crystallinity of the phases. Small intensity variations are due

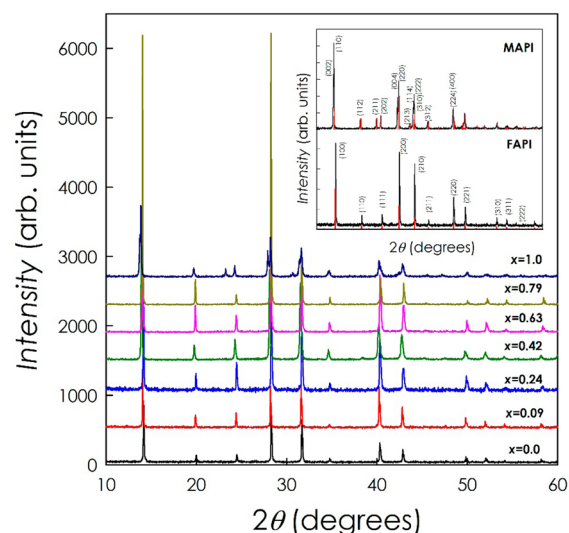


Figure 2. XRD patterns for samples of the $\text{FA}_{1-x}\text{MA}_x\text{PbI}_3$ solid solution. Patterns are vertically shifted to clarify viewing. Inset: XRD patterns of the two end members of the solid solution, namely, FAPI and MAPI, together with the reflection positions from the literature patterns and Miller indices (red vertical bars).

211 to possible preferential orientation effects during sample
 212 preparation.

213 It is interesting to observe that even a small amount of the
 214 larger FA cation (ionic radii have been estimated to be 253 and
 215 217 pm for FA and MA, respectively¹⁶) in the solid solution, as
 216 in the $x = 0.79$ sample, gave rise, at the end of the synthesis, to
 217 a sample with the cubic crystal structure. Moreover, for the low-
 218 MA-containing samples, black perovskite samples were
 219 obtained at the end of the synthesis without the need for any
 220 thermal treatment, as in the case of the pure FAPI sample. This
 221 means that very low MA contents, such as in the $x = 0.09$
 222 sample, are already able to destabilize the hexagonal phase.
 223 However, as shown later in the text, for small x values, the
 224 perovskite phase is not stable with time. By using the effective
 225 radii of the organic cations, $r_{\text{eff}} = 217$ pm for MA and $r_{\text{eff}} = 253$
 226 pm for FA, to calculate a tolerance factor, it was found that $\alpha =$
 227 0.91 for MAPbI_3 versus 0.98 for FAPbI_3 .⁹ Both values should
 228 give a perovskite structure that can be observed for $0.81 < \alpha <$
 229 1.01, which is not the case for δ - FAPbI_3 . It is clear that the
 230 spherical approximation used to estimate the effective radii of
 231 the organic cations is too simplistic in the present case and that
 232 the shape and hydrogen-bonding capabilities of each organic
 233 species play crucial roles in the definition of the structural
 234 properties of these hybrid perovskites.⁹

235 Panels a and b of [Figure 3](#) show the trends in the cell volume
 236 (V) and cubic lattice parameter, respectively, of the
 237 $\text{FA}_{1-x}\text{MA}_x\text{PbI}_3$ solid solution, as obtained from Rietveld
 238 refinement of the diffraction data, as a function of the x
 239 value. The data are reported as cell volumes per formula unit,
 240 considering that the $Pm\bar{3}m$ and the $I4mc$ space groups have
 241 different Z values. In the [Supporting Information](#) are reported
 242 the values of a and V as obtained from the Rietveld refinement
 243 of the patterns, together with an illustrative refined pattern.

244 [Figure 4](#) shows the differential scanning calorimetry (DSC)
 245 measurements for all of the samples except MAPI between -90
 246 and 200 °C (from -90 to 100 °C for MAPI), showing the
 247 well-known tetragonal-to-cubic phase transition for MAPI at
 248 about 57 °C and the hexagonal-to-cubic phase transition for the

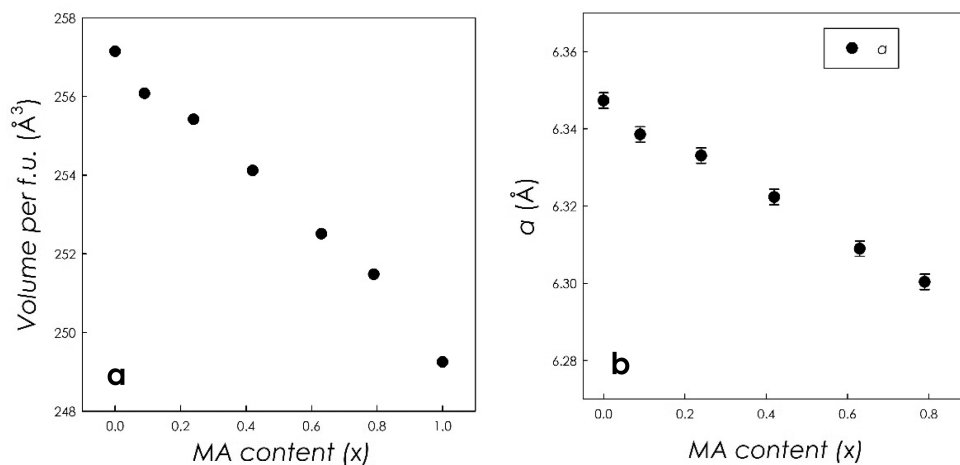


Figure 3. (a) Cell volume and (b) cubic lattice parameter of the $\text{FA}_{1-x}\text{MA}_x\text{PbI}_3$ solid solution as functions of x .

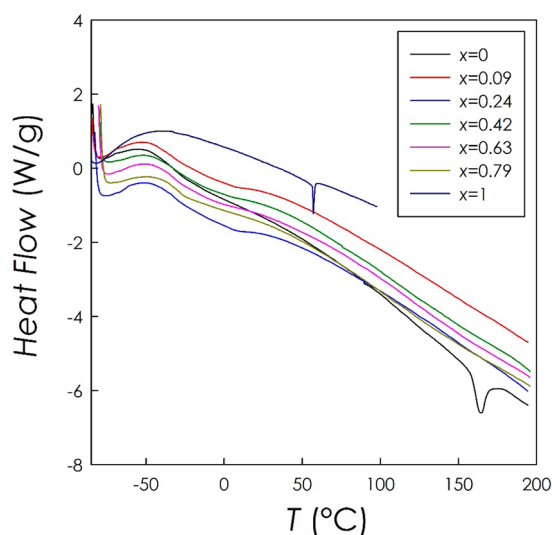


Figure 4. DSC measurements of samples of the $\text{FA}_{1-x}\text{MA}_x\text{PbI}_3$ solid solution. Data for MAPI have been shifted by +1 to clarify the view of the peak corresponding to the tetragonal-to-cubic phase transition.

249 as-prepared yellow FAPI at about 165 °C. As expected and in
 250 agreement with the XRD results, none of the intermediate
 251 compositions present any peaks in the investigated temperature
 252 range because the perovskite phase was stabilized by the
 253 doping. The results for the thermal stability of the
 254 $\text{FA}_{1-x}\text{MA}_x\text{PbI}_3$ solid solution, determined by means of DSC
 255 and not yet reported in the current literature, indicate that the
 256 absence of phase transitions is a beneficial aspect of the use of
 257 these mixed phases.

258 Returning to the data of Figure 3, one can see that linear
 259 decreases of both the cell volume (Figure 3a) and the cubic a
 260 lattice parameter (Figure 3b) occurred with increasing amount
 261 of the smaller MA cation in the solid solution (about 3%
 262 volume shrinkage). This behavior is consistent with Vegard's
 263 law of solid solution formation, which could be anticipated for
 264 this system but which is confirmed by the present structural
 265 data, DSC data, and optical absorbance results (see later in the
 266 text). Other recent literature results based on thin films have
 267 indicated slightly different trends. A nonlinear trend, for
 268 example, was found in ref 3, where, for example, the $x = 0$
 269 and 0.2 samples had the same cell volume and a significant

decrease of V was found for the $x = 0.8$ sample. Binek and co-
 270 workers considered the doping of the FAPI phase with 5%,
 271 10%, and 15% MA cation, and their mixed samples, after
 272 synthesis, were rich in the hexagonal FAPI phase for all doping
 273 levels, a with reduction in the amount of this phase with
 274 increasing methylammonium doping.⁶ In their article, they
 275 indicated no shrinkage of the unit cell upon the replacement of
 276 FA with MA, even for stoichiometries up to about $x = 0.13$. It is
 277 important to emphasize that, in both of the works cited here,
 278 the thin-film samples were prepared by immersion of the
 279 substrate in mixed FAI/MAI solutions and cannot be directly
 280 compared to the powdered samples prepared and characterized
 281 by the synthetic method used in the present work. In particular,
 282 whereas the synthetic approach used herein provides strict
 283 control over the stoichiometry, the earlier methods can lead to
 284 phases with different stoichiometries. However, the results
 285 reported in this work can be used as a reference to rationalize
 286 the results obtained for thin films.
 287

The stability as a function of time of FAPI (black)
 288 perovskites is well-known and was investigated previously.⁶ In
 289 general, once the α -phase has been stabilized by thermal
 290 annealing at about 180–185 °C, this phase remains stable in
 291 the black form for several days with the progressive formation
 292 of the yellow hexagonal phase, which is usually observed after
 293 10 days regardless of storage in a vacuum or inert gas.⁶
 294 However, no data are actually available on the time stability of
 295 mixed MA/FA systems, which are considered to be very
 296 efficient absorbers for use in PSCs. Figure 5 reports the XRD
 297 patterns of the $x = 0$ (FAPI), $x = 0.09$, and $x = 0.24$ samples
 298 immediately after synthesis and after 10 days of storage in a
 299 glovebox and in dark glass containers (aged samples). The blue
 300 vertical bars in the plot correspond to the reference pattern for
 301 the black α -FAPI, whereas the orange vertical bars correspond
 302 to the hexagonal δ -FAPI reference pattern.
 303

FAPI developed a remarkable amount of hexagonal phase
 304 after the considered time frame, in agreement with previous
 305 data. $\text{FA}_{0.91}\text{MA}_{0.09}\text{PbI}_3$ also developed a significant fraction of
 306 the δ -phase, whereas for $\text{FA}_{0.76}\text{MA}_{0.24}\text{PbI}_3$, the amount of the δ -
 307 phase was very small. For stoichiometries with $x > 0.24$, no
 308 traces of the hexagonal phase were detected. It should be noted
 309 that these preliminary results are related to optimal storage
 310 conditions and relatively short-time evaluations after synthesis.
 311 However, this evidence strongly suggests that, whereas the
 312 complete substitution of FA by MA (or other cations) directly
 313

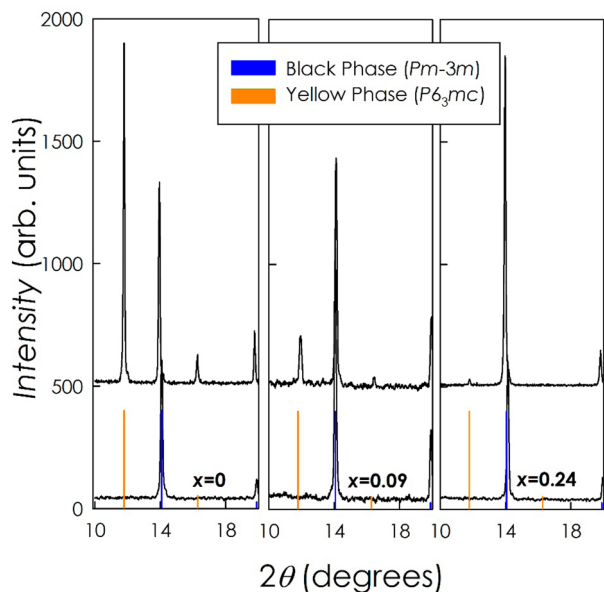


Figure 5. XRD patterns of the $x = 0, 0.09,$ and 0.24 samples of the $\text{FA}_{1-x}\text{MA}_x\text{PbI}_3$ solid solution (bottom) immediately after synthesis and (top) after 10 days of storage. Orange and blue vertical bars correspond to the reference patterns of the hexagonal and cubic structures, respectively, of FAPI.

314 stabilizes the (cubic) perovskite phase at room temperature
 315 after the synthesis, care must be taken when considering the
 316 stability of MA/FA mixed phases. In fact, in this work, we have
 317 shown that the time stability of cubic FAPI-based lattices
 318 stabilized by low cation replacement might be poor. This
 319 suggests that other mixed systems such as Cs-doped and I-/Br-
 320 doped FAPI perovskites should be re-evaluated concerning
 321 their phase stability with time.^{17,18}

322 For the samples investigated in this work, optical measure-
 323 ments were carried out to define the band-gap values as a
 324 function of (real) stoichiometries. The vis-NIR diffuse
 325 reflectance spectra and the trends in the band gaps as functions
 326 of x are reported in panels a and b, respectively, of Figure 6.
 327 [The $x = 0$ (FAPI) values refer to the cubic “black” phase.] The
 328 E_g values were obtained from the extrapolation of the linear
 329 part of $[F(R)h\nu]^2$, where $F(R)$ is the Kubelka–Munk function
 330 $F(R) = (1 - R)^2/2R$.^{19,20}

331 FAPI perovskite was found to have a band-gap value of about
 332 1.48 eV, in agreement with the literature, and with increasing
 333 amount of MA, the E_g value increased to about 1.53 eV (again

in agreement with previously reported values), thus indicating a
 334 relatively small shift with MA substitution for FA in the
 335 $\text{FA}_{1-x}\text{MA}_x\text{PbI}_3$ solid solution.^{1,4,7}

336
 337 Figure 6c reports the evolution of the diffuse reflectance
 338 spectra of aged samples, analogous to those presented in Figure
 339 5 for the XRD characterization. It can be observed that, for $x =$
 340 0 and 0.09, the spectra showed a shift of the band gap to higher
 341 values when the samples were left under optimal storage
 342 conditions for several days. On the other hand, for the sample
 343 with $x = 0.24$ and greater, there was no shift of the band gap
 344 (the dotted curve is exactly superimposed on the solid curve for
 345 the as-prepared sample), suggesting a greater stability of the
 346 material, at least in this time frame. The results for the optical
 347 measurements of aged samples are in very good agreement with
 348 the phase separation observed for the aged samples by means of
 349 XRD: The samples exhibiting a shift to higher values of E_g are
 350 the same as those showing the separation of the hexagonal δ -
 351 phase with time (see Figure 5). This agreement clearly indicates
 352 that the time variation of the optical properties of the samples
 353 within the $\text{FA}_{1-x}\text{MA}_x\text{PbI}_3$ solid solution can be directly
 354 correlated with the phase stability of the same samples and
 355 that this change in the absorption properties might have a
 356 crucial effect on the performance of PSCs employing such
 357 materials as absorbing layers. It should be noted that, for low x
 358 values, the degradation was found to be very fast (within a few
 359 days under optimal storage conditions) and that, for samples
 360 with higher x values, the same behavior might also occur at
 361 longer times. Further investigation in this regard is strongly
 362 needed for most of the mixed doped systems of hybrid
 363 perovskites. Finally, based on the observation of an increase in
 364 band-gap values due to phase separation within the samples, it
 365 can be suggested that literature data where the band-gap values
 366 for FAPI samples are reported to be very high and on the order
 367 of 1.53–1.55 eV might be due to significant phase separation
 368 occurring within the samples.

CONCLUSIONS

369
 370 In this work, we have deeply investigated the $\text{FA}_{1-x}\text{MA}_x\text{PbI}_3$
 371 system, defining its crystal structure, phase stability, and optical
 372 properties as functions of the actual x values determined by
 373 means of solid-state NMR spectroscopy. The collected results
 374 confirm the formation of a solid solution within this mixed
 375 system. By properly controlling the relative MA and FA
 376 amounts, we obtained reliable evidence of structural changes
 377 occurring upon doping. In addition, we characterized the time
 378 stability of mixed systems, highlighting a phase separation

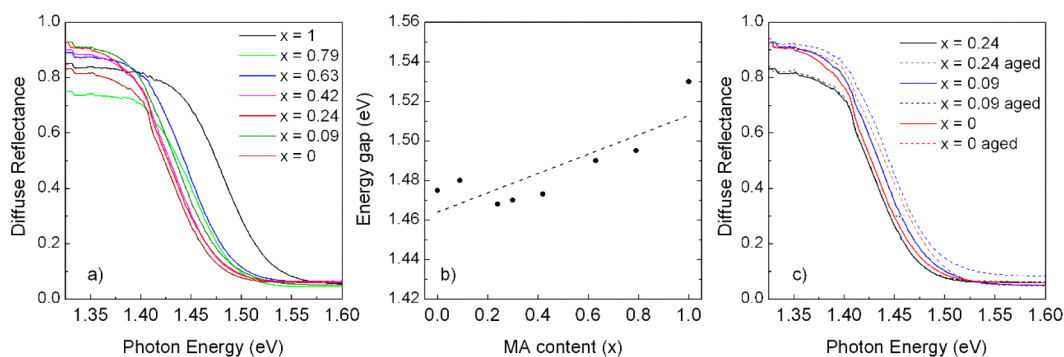


Figure 6. (a) Diffuse reflectance spectra for the $\text{FA}_{1-x}\text{MA}_x\text{PbI}_3$ solid solution; (b) trend in the energy gap as a function of x for the $\text{FA}_{1-x}\text{MA}_x\text{PbI}_3$ solid solution; and (c) diffuse reflectance spectra of as-prepared and aged samples for $x = 0$ (FAPI), 0.09, and 0.24.

379 phenomena in aged samples leading to the formation of the δ -
380 phase. The optical properties were also found to scale with the
381 real x values, and the time degradation of the samples resulted
382 in an increase of the band-gap values due to the phase
383 separation observed by diffraction. These results, providing a
384 reliable definition of structure–property correlations in the
385 $\text{FA}_{1-x}\text{MA}_x\text{PbI}_3$ system for well-defined doping levels, demon-
386 strate the significant stability issue of such mixed systems that
387 could also be a key issue for other mixed systems based on
388 FAPI perovskite. These effects might, in turn, have detrimental
389 effects on the performance of PSCs based on these materials as
390 active layers.

391 ■ ASSOCIATED CONTENT

392 ● Supporting Information

393 The Supporting Information is available free of charge on the
394 ACS Publications website at DOI: 10.1021/acs.jpcc.7b01250.

395 Table reporting the structural data for the $\text{FA}_{1-x}\text{MA}_x\text{PbI}_3$
396 solid solution ($x = 0, 0.09, 0.24, 0.42, 0.63, 0.79, \text{ and } 1.0$)
397 as determined from the Rietveld refinement of the
398 patterns and illustrative refined pattern for FAPI (PDF)

399 ■ AUTHOR INFORMATION

400 Corresponding Author

401 *E-mail: lorenzo.malavasi@unipv.it. Tel.: +39 382 987921.

402 ORCID

403 Paolo Quadrelli: 0000-0001-5369-9140

404 Lorenzo Malavasi: 0000-0003-4724-2376

405 Notes

406 The authors declare no competing financial interest.

407 ■ ACKNOWLEDGMENTS

408 The authors gratefully acknowledge project PERSEO “Perrov-
409 skite-Based Solar Cells: Towards High Efficiency and Long-
410 Term Stability” [Bando PRIN 2015-Italian Ministry of
411 University and Scientific Research (MIUR) Decreto Direttor-
412 iale 4 Novembre 2015 no. 2488, Project 2015SLECAJ] for
413 funding.

414 ■ REFERENCES

- 415 (1) Jeon, N. J.; Noh, J. H.; Yang, W. S.; Kim, Y. C.; Ryu, S.; Seo, J.;
416 Seok, S., II Compositional engineering of perovskite materials for high-
417 performance solar cells. *Nature* **2015**, *517*, 476.
- 418 (2) Pellet, N.; Gao, P.; Gregori, G.; Yang, T.-Y.; Nazeeruddin, M. K.;
419 Maier, J.; Graetzel, M. Mixed-organic-cation perovskite photovoltaics
420 for enhanced solar-light harvesting. *Angew. Chem., Int. Ed.* **2014**, *53*,
421 3151.
- 422 (3) Jacobsson, T. J.; Correa-Baena, J.-P.; Pazoki, M.; Saliba, M.;
423 Schenk, K.; Graetzel, M.; Hagfeldt, A. Exploration of the composi-
424 tional space for mixed lead halogen perovskites for high efficiency solar
425 cells. *Energy Environ. Sci.* **2016**, *9*, 1706.
- 426 (4) Yang, W. S.; Noh, J. H.; Jeon, N. J.; Kim, Y. C.; Ryu, S.; Seo, J.;
427 Seok, S. II High-performance photovoltaic perovskite layers fabricated
428 through intramolecular exchange. *Science* **2015**, *348*, 1234.
- 429 (5) Han, Q.; Bae, S.-H.; Sun, P.; Hsieh, Y.-T.; Yang, Y.; Rim, Y. S.;
430 Zhao, H.; Chen, Q.; Shi, W.; Li, G.; et al. Single crystal formamidinium
431 lead iodide (FAPbI_3): insight into the structural, optical, and electrical
432 properties. *Adv. Mater.* **2016**, *28*, 2253–2258.
- 433 (6) Binek, A.; Hanusch, F. C.; Docampo, P.; Bein, T. Stabilization of
434 the trigonal high-temperature phase of formamidinium lead iodide. *J.*
435 *Phys. Chem. Lett.* **2015**, *6*, 1249.

(7) Lee, J.-W.; Seol, D.-J.; Cho, A.-N.; Park, N.-G. High-efficiency
perovskite solar cells based on the black polymorph of HC-
 $(\text{NH}_2)_2\text{PbI}_3$. *Adv. Mater.* **2014**, *26*, 4991.

(8) Yang, Z.; Chueh, C.-C.; Liang, P.-W.; Crump, M.; Lin, F.; Zhu,
Z.; Jen, A. K.-Y. Effects of formamidinium and bromide ion
substitution in methylammonium lead triiodide toward high-perform-
ance perovskite solar cells. *Nano Energy* **2016**, *22*, 328–337.

(9) Weber, O. J.; Charles, B.; Weller, M. T. Phase behaviour and
composition in the formamidinium–methylammonium hybrid lead
iodide perovskite solid solution. *J. Mater. Chem. A* **2016**, *4*, 15375.

(10) Mancini, A.; Quadrelli, P.; Amoroso, G.; Milanese, C.; Boiocchi,
M.; Sironi, A.; Patrini, M.; Guizzetti, G.; Malavasi, L. Synthesis,
structural and optical characterization of APbX_3 (A = methylammo-
nium, dimethylammonium, trimethylammonium; X = I, Br, Cl) hybrid
organic-inorganic materials. *J. Solid State Chem.* **2016**, *240*, 55.

(11) Mancini, A.; Quadrelli, P.; Milanese, C.; Patrini, M.; Guizzetti,
G.; Malavasi, L. $\text{CH}_3\text{NH}_3\text{Sn}_x\text{Pb}_{1-x}\text{Br}_3$ hybrid perovskite solid solution:
synthesis, structure, and optical properties. *Inorg. Chem.* **2015**, *54*,
8893.

(12) Rodriguez-Carvajal, J. Recent advances in magnetic structure
determination by neutron powder diffraction. *Phys. B* **1993**, *192*, 55.

(13) Massiot, D.; Fayon, F.; Capron, M.; King, I.; Le Calve, S.;
Alonso, B.; Durand, J. O.; Bujoli, B.; Gan, Z.; Hoatson, G. Modelling
one- and two-dimensional solid-state NMR spectra. *Magn. Reson.*
Chem. **2002**, *40*, 70.

(14) Fu, Y.; Zhu, H.; Schrader, A. W.; Liang, D.; Ding, Q.; Joshi, P.;
Hwang, L.; Zhu, X.-Y.; Jin, S. Nanowire lasers of formamidinium lead
halide perovskites and their stabilized alloys with improved stability.
Nano Lett. **2016**, *16*, 1000.

(15) Baikie, T.; Barrow, N. S.; Fang, Y.; Keenan, P. J.; Slater, P. R.;
Piltz, R. O.; Gutmann, M.; Mhaisalkar, S. G.; White, T. J. A combined
single crystal neutron/X-ray diffraction and solid-state nuclear
magnetic resonance study of the hybrid perovskites $\text{CH}_3\text{NH}_3\text{PbX}_3$
(X = I, Br and Cl). *J. Mater. Chem. A* **2015**, *3*, 9298–9307.

(16) Kieslich, G.; Sun, S.; Cheetham, A. K. An extended tolerance
factor approach for organic–inorganic perovskites. *Chem. Sci.* **2015**, *6*,
3430.

(17) Rehman, W.; Milot, R. L.; Eperon, G. E.; Wehrenfennig, C.;
Boland, J. L.; Snaith, H. J.; Johnston, M. B.; Herz, L. M. Charge-carrier
dynamics and mobilities in formamidinium lead mixed-halide
perovskites. *Adv. Mater.* **2015**, *27*, 7938–7944.

(18) Yi, C.; Luo, J.; Meloni, S.; Boziki, A.; Ashari-Astani, N.; Graetzel,
C.; Zakeeruddin, S. M.; Roethlisberger, U.; Graetzel, M. Entropic
stabilization of mixed A-cation ABX_3 metal halide perovskites for high
performance perovskite solar cells. *Energy Environ. Sci.* **2016**, *9*, 656–
662.

(19) Kubelka, P.; Munk, F. Ein Beitrag zur Optik der farbanstriche. *Z.*
Techn. Phys. **1931**, *12*, 593–601.

(20) Kim, H.-S.; Lee, C.-R.; Im, J.-H.; Lee, K.-B.; Moehl, T.;
Marchioro, A.; Moon, S.-J.; Humphry-Baker, R.; Yum, J.-H.; Moser, J.
E.; et al. Lead iodide perovskite sensitized all-solid-state submicron
thin film mesoscopic solar cell with efficiency exceeding 9%. *Sci. Rep.*
2012, *2*, 591.